

Performance of Imaging Receivers using Convex Lens in Indoor MIMO VLC Systems

K. V. S. Sai Sushanth and A. Chockalingam

Department of ECE, Indian Institute of Science, Bangalore 560012, India

Abstract—In multiple-input multiple-output (MIMO) indoor visible light communication (VLC) systems that employ non-imaging receivers, the bit error performance is degraded due to high spatial correlation. Imaging receivers can mitigate this degradation by concentrating the light energy, thereby reducing the correlation among the elements in the channel matrix. In this paper, we investigate the performance of the state-of-the-art MIMO VLC modulation schemes with *convex lens-based imaging receivers*. The MIMO modulation schemes considered include the well known spatial multiplexing (SMP) as well as other more recently proposed schemes such as generalized spatial modulation (GSM), quad-LED complex modulation (QCM), and dual-LED complex modulation (DCM). Performance gains up to 68 dB at 10^{-5} bit error rate are shown to be achieved with a convex lens based imaging receiver compared to a non-imaging receiver. We also study the spatial distribution of the best performing modulation scheme based on a minimum euclidean distance based metric. Results show that, with convex lens based imaging receiver, QCM and DCM outperform GSM and SMP.

Keywords – Visible light communication, MIMO modulation, spatial correlation, imaging receivers, convex lens.

I. INTRODUCTION

Visible light communication (VLC) technology is emerging as an attractive alternative to RF communication technology for wireless communication in indoor environments [1]. In VLC systems, signals are transmitted wirelessly in visible light wavelengths (400nm to 700nm) using light emitting diodes (LED) at the transmitter and the received signals are detected at the receiver using photo diodes (PD). An important advantage of VLC is its ability to simultaneously provide both energy-efficient lighting as well as high data rate communications. Other advantages include low cost, no spectrum licensing issues, and security in closed-room applications.

Intensity modulation (IM) of the LED at the transmitter and direct detection (DD) at the receiver are widely used in VLC systems. Hence the signals modulating the LED in VLC are real and non-negative. Signaling using multiple-input multiple-output (MIMO) techniques is an attractive way to increase spectral efficiency in VLC systems [2]-[4]. In MIMO VLC systems, analogous to using multiple antennas at the transmitter and receiver in MIMO RF communications, multiple LEDs and multiple PDs are used at the VLC transmitter and receiver, respectively. MIMO VLC modulation schemes popularly considered in the literature include spatial multiplexing (SMP), space shift keying (SSK) and its generalization, spatial modulation (SM)/optical spatial modulation (OSM), and generalized spatial modulation (GSM) [2]-[4]. More recent MIMO VLC modulation schemes include quad-LED complex modulation (QCM) and dual-LED complex modulation (DCM) [5].

This work was supported in part by the J. C. Bose National Fellowship, Department of Science and Technology, Government of India.

While MIMO techniques are attractive to achieve increased data rates and spectral efficiencies, MIMO VLC systems suffer from the problem of high spatial correlation in MIMO VLC channels. The correlations between the elements of the channel matrix depend on the system configuration/parameters including spatial positions of the transmitter (LEDs) and the receiver (PDs), inter-LED spacing, inter-PD spacing, radiation pattern of the LEDs, field-of-view (FOV) of the PDs, etc. High channel correlation is a key cause for significant degradation in MIMO VLC system performance. Use of imaging receivers can alleviate this performance degradation [6]-[9]. In imaging receivers, the signals from different light sources are demultiplexed at the receiver with the help of an imaging lens so that correlation in the channel gain matrix is reduced.

Imaging receivers with different types of lens such as convex lens, hemispherical lens, and fish-eye lens have been studied in the literature [6],[7],[9]. Most of these studies, however, have considered mainly SMP and SM with imaging receivers. More recent modulation schemes such as GSM, QCM, and DCM have been shown better performance compared to SMP and SM [4],[5]. However, the performance of GSM, QCM, and DCM have not been studied in the presence of imaging receivers. Our new contribution in this paper is that we study the performance of GSM, QCM, and DCM with a convex lens based imaging receiver (which has not been reported in the literature) and compare them with that of SMP. Our results show that a performance gain of up to 68 dB at 10^{-5} bit error rate (BER) can be achieved with a convex lens based imaging receiver compared to a non-imaging receiver. We also present an analytical framework to capture the dependence of the performance of various modulation schemes on the spatial positions of the receiver by using minimum euclidean distance of the received signal set as a performance measure in high SNR region. Using this framework, we obtain the spatial distribution of the best performing modulation scheme with non-imaging as well as convex lens based imaging receiver. Our results show QCM and DCM with convex lens based imaging receiver outperform SMP and GSM with the same imaging receiver.

II. CONVEX LENS BASED IMAGING RECEIVER

Consider an indoor MIMO VLC system consisting of N_t luminaires, where each luminaire provides illumination as well as transmits data. The geometric setup of the considered MIMO VLC system with convex imaging lens based receiver is shown in Fig. 1. A room of size $5\text{m} \times 5\text{m} \times 3.5\text{m}$ is considered. The luminaire plane is located at a height of 0.5m below the ceiling and the N_t luminaires are separated by a distance of d_{tx} from each other in this plane. The receiver plane is located at a height of 0.5m from the ground. Each

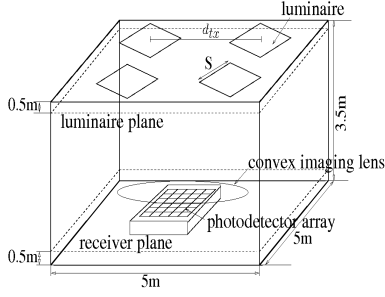


Fig. 1. Indoor MIMO VLC system model with convex lens imaging receiver.

luminaire consists of an array of LEDs arranged such that the luminaire's illumination surface is a square with side length S . The LEDs inside the luminaire emit unpolarized white light with lambertian radiation pattern and also perform the conversion of data from electrical to optical domain. In a given channel use, a luminaire is either OFF (zero intensity level) or radiate light with certain intensity level based on the MIMO modulation scheme used. The transmit signal vector \mathbf{x} of dimension $N_t \times 1$ is $\mathbf{x} = [x_1 \ x_2 \ \dots \ x_{N_t}]^T$, where x_j denotes the light intensity emitted by the j th luminaire. At the receiver side, a convex imaging lens is used along with a PD array to receive the optical signals. The PD array consists of N_r PDs and is placed at the focal plane of the imaging lens such that the center of the PD array lies below the centroid of the aperture of the imaging lens (see Figs. 2, 3). The lens focuses the luminaires onto the PD array and the image of a luminaire on the PD array is defined as a spot. The size of the PD array is chosen such that the spot of each luminaire falls on the PD array for every receiver location inside the room.

Consider the j th luminaire with four corner points A, B, C, D as shown in the Fig. 2. Let C_I at location $(x_{C_I}, y_{C_I}, z_{C_I})$ be the centroid of the aperture of imaging lens. The projection of the j th luminaire on the PD array is a spot with corners A', B', C', D' . Let the coordinates of point A be (x_A, y_A, z_A) . Then the coordinates of the point A' are given by

$$x_{A'} = x_{C_I} - M_j(x_A - x_{C_I}), \quad (1)$$

$$y_{A'} = y_{C_I} - M_j(y_A - y_{C_I}), \quad (2)$$

$$z_{A'} = z_{C_I} - M_j(z_A - z_{C_I}), \quad (3)$$

where M_j is the magnification factor of the imaging lens for the j th luminaire which is given by

$$M_j = \begin{cases} f/(d_j^z - f), & \text{if } \theta_j \leq FOV \\ 0, & \text{otherwise,} \end{cases} \quad (4)$$

where f is the focal length of the convex lens, d_j^z is the distance between the j th luminaire and the lens along the z -axis (vertical axis), θ_j is the angle of incidence of the j th luminaire at the aperture of the lens, and FOV is the field-of-view angle of the PD. The side length of the j th luminaire is S (i.e., the distance between the corner points B and C). The side length of the spot corresponding to the j th luminaire is given by $S' = M_j S$. While the size of the spot corresponding to a luminaire depends on the magnification factor and the side length of that luminaire, its position on PD array depends on the receiver location, distance between the luminaires, and

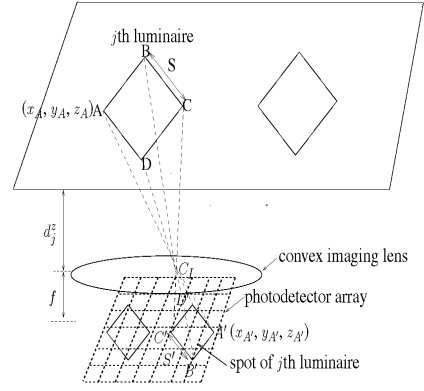


Fig. 2. Schematic showing the imaging of a luminaire on the PD array using convex lens.

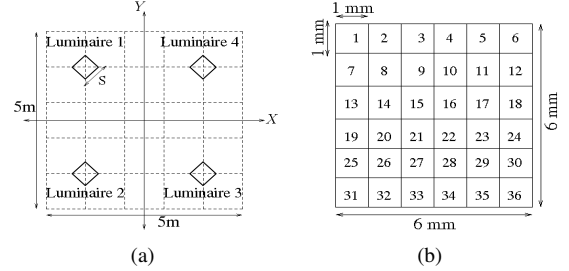


Fig. 3. (a) Position of various luminaires on the luminaire plane. (b) PD array with $N_r = 36$ used in convex lens based imaging receiver.

the magnification factor. The line-of-sight (LOS) channel gain between the j th luminaire and centroid of the aperture of the lens, denoted by h_j^{LOS} , is given by

$$h_j^{LOS} = \frac{m+1}{2\pi} \cos^m \phi_j \cos \theta_j \frac{A_L}{d_j^2} \text{rect}\left(\frac{\theta_j}{FOV}\right), \quad (5)$$

where d_j is the LOS distance between the centroid of the j th luminaire (L_j) and the centroid of the aperture of the lens (C_I), ϕ_j is the angle of emergence at the j th luminaire with respect to the normal at L_j , θ_j is the angle of incidence at C_I , m is the mode number of the radiating lobe given by $m = \frac{-\ln(2)}{\ln \cos \Phi_{\frac{1}{2}}}$, $\Phi_{\frac{1}{2}}$ is the half-power semi-angle of the LEDs inside the luminaire, A_L is the aperture area of the lens, FOV is the field-of-view of the PD, and $\text{rect}(x) = 1$, if $|x| \leq 1$, and $\text{rect}(x) = 0$, if $|x| > 1$, where $|\cdot|$ denotes the absolute value operator (or the cardinality of a set).

Let spot j be the spot corresponding to j th luminaire on the PD array. Let h_{ij}^M be the channel gain between the j th luminaire and i th PD due to the imaging lens [8], which is defined as the ratio of the area of spot j that falls on the i th PD to the total area of spot j on the PD array, i.e.,

$$h_{ij}^M = \frac{\text{Area}(\text{spot } j \cap \text{ith PD})}{\text{Area}(\text{spot } j)}. \quad (6)$$

The net channel gain between the j th luminaire and i th PD, denoted by h_{ij} , can be defined as the ratio of total optical power received by the i th PD to the total optical power transmitted by j th luminaire, and is given by $h_{ij} = h_{ij}^M h_j^{LOS}$. The $N_r \times 1$ received vector \mathbf{y} at the receiver (in the electrical domain) is given by

$$\mathbf{y} = \mathbf{aH}\mathbf{x} + \mathbf{n}, \quad (7)$$

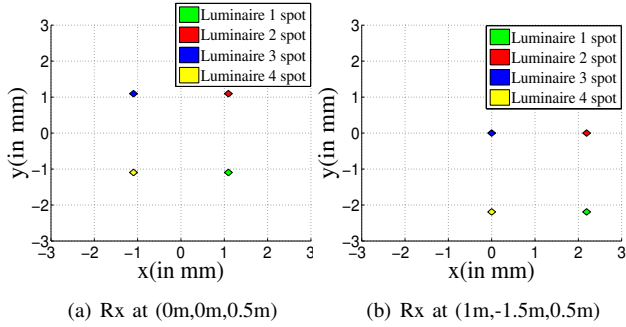


Fig. 4. Spots obtained on the PD array using convex imaging lens at different receiver locations.

Room	Length \times Width \times Height	5m \times 5m \times 3.5m
Transmitter	No. of luminaires (N_t)	4
	Side length of luminaire (S)	17.68cm
	Height from the floor	3m
	Half-power semi-angle ($\Phi_{\frac{1}{2}}$)	60°
	Mode number, m	1
	Inter-luminaire distance (d_{tx})	3m
	Convex lens based imaging rx.	No. of PDs
PD dimensions in PD array		1mm \times 1mm
Field-of-view (FOV)		85°
Responsivity of PD (a)		0.4 Amp/Watt
Focal length of the lens (f)		1.825mm
Aperture area of the lens (A_L)		1mm ²

TABLE I
INDOOR MIMO VLC SYSTEM PARAMETERS.

where a is the responsivity of the PD, \mathbf{H} is the $N_r \times N_t$ channel gain matrix whose entry in the i th row and j th column is h_{ij} , and $\mathbf{n} = [n_1 \ n_2 \ \dots \ n_{N_r}]$ is the noise vector. The optical intensity values of the x_i s in \mathbf{x} are determined by the modulation scheme used. The electrical-to-optical conversion factor is assumed to be unity. The optical-to-electrical conversion factor at the receiver is given by the responsivity a Amp/Watt. The electrical noise n_i s in \mathbf{n} are modeled as i.i.d. real AWGN with zero mean and variance σ^2 . The SNR at a PD (in the electrical domain) is defined as $\frac{(aP_r)^2}{\sigma^2}$, where P_r is the total received optical power and σ^2 is the total noise power at a PD. The total power received at the i th PD is given by $(\mathbf{H}_i \mathbf{x})^2$. Therefore, the average received optical power is given by $\mathbb{E}\{\|\mathbf{H}\mathbf{x}\|^2\} = \frac{1}{N_r} \sum_{i=1}^{N_r} \mathbb{E}\{(\mathbf{H}_i \mathbf{x})^2\}$, where \mathbf{H}_i is the i th row of \mathbf{H} , $\mathbb{E}\{\cdot\}$ is the expectation w.r.t. the signal vector \mathbf{x} . Hence, the average SNR at the receiver in the electrical domain is given by $\bar{\gamma} = \frac{a^2}{\sigma^2 N_r} \sum_{i=1}^{N_r} \mathbb{E}\{(\mathbf{H}_i \mathbf{x})^2\}$.

The system parameters considered for the indoor MIMO VLC system are given in Table I. The size and position of the spot on the PD array due to a given luminaire can be found using (1)-(4). The spots on the PD array corresponding to different luminaires when the receiver is located at (0m,0m,0.5m) and (1m,-1.5m,0.5m) are shown in Figs. 4(a) and 4(b), respectively. Note that the spots of different luminaires do not overlap on the PD array, leading to correlation reduction in the channel matrix when the convex lens is used at the receiver.

III. MIMO MODULATION SCHEMES

The considered MIMO VLC modulation schemes are described below.

A. SMP scheme: In SMP, N_t positive, real-valued M -ary PAM

symbols are sent simultaneously in a channel use through IM of N_t luminaires. So the achieved rate in SMP is $\eta_{\text{smp}} = N_t \log_2 M$ bpcu, where $M = |\mathbb{M}|$ and $\mathbb{M} = \{I_1, I_2, \dots, I_M\}$ denotes the M -ary alphabet where the intensity of the m th symbol in the alphabet is given by $I_m = \frac{2I_{\text{ave}}m}{M+1}$, $m = 1, 2, \dots, M$, where I_{ave} is the average intensity level. For example, if $I_{\text{ave}} = 1$, the 4-ary PAM signal set is given by $\mathbb{M} = \{\frac{2}{5}, \frac{4}{5}, \frac{6}{5}, \frac{8}{5}\}$.

B. GSM scheme: In GSM, N_a out of N_t luminaires are activated in a channel use [4]. The selection of which N_a luminaires are activated in a channel use is made based on $\lfloor \log_2 \binom{N_t}{N_a} \rfloor$ bits. The activated luminaires transmit with intensity levels taken from the M -ary PAM alphabet, \mathbb{M} . The remaining $N_t - N_a$ luminaires transmit zero intensity values (i.e., they remain OFF). So the achieved rate in GSM is $\eta_{\text{gsm}} = \lfloor \log_2 \binom{N_t}{N_a} \rfloor + N_a \log_2 M$ bpcu.

C. QCM scheme: In QCM, one complex modulation symbol is sent in a channel use using four luminaires [5]. Let \mathbb{A} denote a complex modulation alphabet (e.g., QAM) and $s \in \mathbb{A}$ denote the complex modulation symbol to be signaled in a given channel use. The symbol s can be written in the form $s = s_I + js_Q$, where s_I and s_Q are the real and imaginary parts of s , respectively. Of the four luminaires, two luminaires (say, Luminaire 1 and Luminaire 2) convey the magnitude and sign of s_I as follows. If $s_I \geq 0$, then Luminaire 1 emits intensity s_I ; if $s_I < 0$, Luminaire 2 emits intensity $|s_I|$. Since $s_I \geq 0$ or < 0 , only any one of Luminaire 1 and Luminaire 2 will be ON in a given channel use and the other will be OFF. Therefore, while the magnitude of s_I is conveyed using IM, the sign of s_I is conveyed through spatial modulation (i.e., which among Luminaire 1 and Luminaire 2 is ON). In a similar way, the other two luminaires (Luminaire 3 and Luminaire 4) convey the magnitude and sign of s_Q . *Example:* If $s = 1 - j3$, then Luminaire 1 emits intensity 1, Luminaire 2 is OFF, Luminaire 3 is OFF, and Luminaire 4 emits intensity 3, so that the transmit vector is $\mathbf{x} = [1 \ 0 \ 0 \ 3]^T$.

D. DCM scheme: In DCM, two luminaires are used to send one complex modulation symbol in a given channel use. Polar representation of complex symbols is used so that one luminaire conveys the magnitude and other luminaire conveys the phase of the complex symbol. Let $s \in \mathbb{A}$ be the complex modulation symbol and its polar representation is $s = re^{j\phi}$, where $r = |s|$, $r \in \mathbb{R}^+$ and $\phi = \arg(s)$, $\phi \in [0, 2\pi)$. Luminaire 1 emits intensity r and Luminaire 2 emits intensity ϕ . The transmit vector \mathbf{x} is given by $\mathbf{x} = [r \ \phi]^T$. *Example:* If $s = 3 + j3$, then $r = 3\sqrt{2}$ and $\phi = \pi/4$, so that the transmit vector is $\mathbf{x} = [3\sqrt{2} \ \pi/4]^T$.

E. Minimum distance of received signal sets: In order to evaluate the relative performance of the above modulation schemes at different spatial positions of the receiver across the room, we consider the following metric that captures the high SNR performance of a given modulation scheme. Let $\mathbb{S}_{\text{tx}} = \{\mathbf{x}_1, \mathbf{x}_2, \dots, \mathbf{x}_L\}$ be the set of all possible transmit signal vectors for a given modulation scheme. In the absence of noise, let \mathbb{S}_{rx} denote the corresponding received signal set for a given \mathbf{H} , i.e., $\mathbb{S}_{\text{rx}} = \{\mathbf{H}\mathbf{x}_1, \mathbf{H}\mathbf{x}_2, \dots, \mathbf{H}\mathbf{x}_L\}$. The set of normalized received signal vectors (i.e., vectors in \mathbb{S}_{rx}

normalized by the average received signal power) is given by $\mathbb{S}_{\text{Rx}} = \{\tilde{\mathbf{y}}_1, \tilde{\mathbf{y}}_2, \dots, \tilde{\mathbf{y}}_L\}$, where $\tilde{\mathbf{y}}_i = \frac{\mathbf{H}\mathbf{x}_i}{\sqrt{\frac{1}{LN_r} \sum_{i=1}^L \|\mathbf{H}\mathbf{x}_i\|^2}}$. The normalized minimum distance of the received signal set is

$$\tilde{d}_{\min, \mathbf{H}} = \min_{\tilde{\mathbf{y}}_i, \tilde{\mathbf{y}}_j \in \mathbb{S}_{\text{Rx}}, i \neq j} \|\tilde{\mathbf{y}}_i - \tilde{\mathbf{y}}_j\|. \quad (8)$$

Let $\mathbb{S}_{\text{Tx}}^{(1)}$ and $\mathbb{S}_{\text{Tx}}^{(2)}$ denote the signal sets of two different modulation schemes and $\tilde{d}_{\min, \mathbf{H}}^{(1)}$ and $\tilde{d}_{\min, \mathbf{H}}^{(2)}$ denote their corresponding normalized minimum distances for a given \mathbf{H} . At high SNRs, the BER performance of modulation scheme with signal set $\mathbb{S}_{\text{Tx}}^{(1)}$ will be better than that of the scheme with $\mathbb{S}_{\text{Tx}}^{(2)}$, if $\tilde{d}_{\min, \mathbf{H}}^{(1)} > \tilde{d}_{\min, \mathbf{H}}^{(2)}$. Also, the SNR gap between the BER performance of the two modulation schemes in the high SNR region is given by $20 \log(\tilde{d}_{\min, \mathbf{H}}^{(1)} / \tilde{d}_{\min, \mathbf{H}}^{(2)})$.

IV. RESULTS AND DISCUSSIONS

In this section, we present the BER performance results of MIMO modulation schemes in the presence of non-imaging receiver and convex lens based imaging receiver. The modulation schemes considered for comparison are *i)* SMP: $N_t = 4$, $M = 2$, $I_{\text{avg}} = 1$, *ii)* GSM: $N_t = 4$, $N_a = 2$, $M = 2$, $I_{\text{avg}} = 1$, *iii)* QCM: $N_t = 4$, 16-QAM, *iv)* DCM: $N_t = 2$, 16-QAM, the magnitude and phase values are sent through luminaires 1 and 3, respectively. All the above schemes have the same rate of 4 bpcu. Maximum-likelihood (ML) detection scheme is used at the receiver.

BER vs SNR performance: The BER performance of the MIMO modulation schemes with non-imaging receiver located at (0m,0m,0.5m) is shown in Fig. 5. In this figure, we plot the simulated BER as well as the analytical upper bound on BER (obtained using union bounding [4]). At moderate-to-high SNRs, the BER upper bounds for all the schemes are found to be very tight. For the case of non-imaging receiver, the performance of the MIMO schemes suffer due to high correlation among the elements of channel gain matrix. In QCM, DCM, and GSM only two luminaires are activated in a channel use, whereas in SMP, all the four luminaires are activated simultaneously to transmit data. Hence the SMP performs worst among all the schemes as shown in Fig. 5. While spatial indexing conveys information bits in GSM, it conveys the sign of the real and imaginary parts of the QAM symbol in QCM. DCM scheme does not use spatial indexing, and hence the performance of DCM is better than QCM and GSM at low SNRs.

The BER performance of the convex imaging lens based receiver located at (0m,0m,0.5m) is shown in the Fig. 6. In this figure also, the BER upper bounds for all the schemes are very tight at moderate-to-high SNRs. By employing convex imaging lens, the performance of all the modulation schemes has improved when compared to the non-imaging case. This is because of the decorrelation among the elements of channel gain matrix achieved with the help of the convex lens. The performance of QCM, GSM, DCM, and SMP are improved by 36 dB, 36.4 dB, 27.4 dB, and 67.8 dB, respectively. We can observe that SMP and DCM achieve the highest and least performance gains, respectively. This is because SMP is the most affected by spatial interference and spatial correlation in the non-imaging case, and so the benefits of imaging effect by

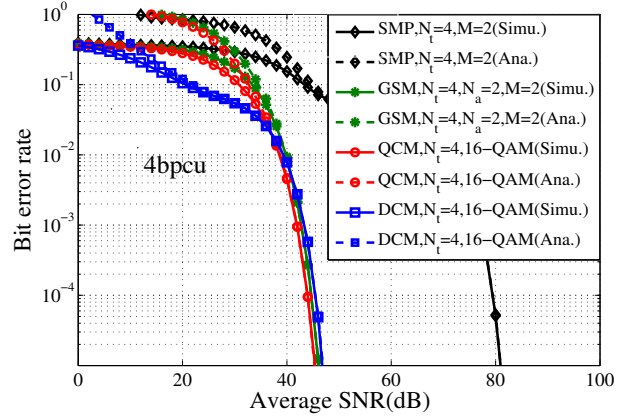


Fig. 5. Analytical upper bound on BER and simulated BER for different MIMO modulation schemes using non-imaging receiver.

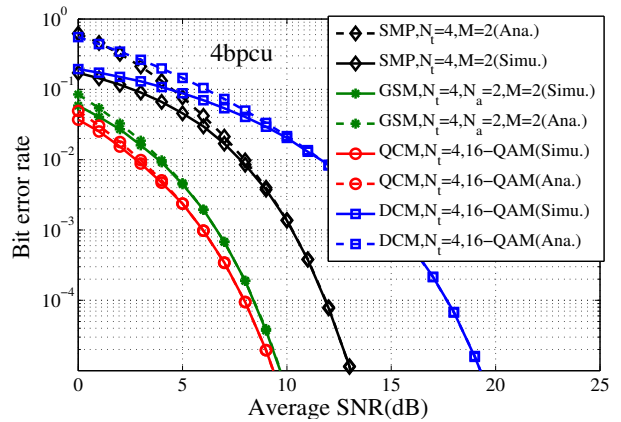


Fig. 6. Analytical upper bound on BER and simulated BER for different MIMO modulation schemes using convex imaging lens based receiver.

the lens is the maximum. Even with this improvement, SMP performs worse than GSM and QCM.

Effect of varying d_{tx} : The BER vs d_{tx} performance of different MIMO modulation schemes using convex imaging lens based receiver at location (0m,0m,0.5m) at 8 dB SNR is shown in Fig. 7. At low d_{tx} values, the spots due to different luminaires get overlapped resulting in non-zero correlation among the elements of channel gain matrix. Hence for all the schemes, the BER is high at low values of d_{tx} . But as d_{tx} increases, the amount of overlap among the spots decreases and the BER performance gets improved. After certain value of d_{tx} , the spots due to different luminaires do not overlap and there is no correlation among the channel gain matrix elements. Hence for $d_{tx} > 0.25\text{m}$, the BER performance remains almost the same. As in Fig. 6, QCM achieves the best performance.

Effect of varying receiver location: As discussed in earlier section, the MIMO scheme with higher $\tilde{d}_{\min, \mathbf{H}}$ value has better BER performance than the one with lower $\tilde{d}_{\min, \mathbf{H}}$ value. The $\tilde{d}_{\min, \mathbf{H}}$ values obtained for different modulation schemes at different receiver locations for convex imaging lens based receiver and non-imaging receiver are presented in Table II. As the receiver location changes, the LOS channel gain changes and so the $\tilde{d}_{\min, \mathbf{H}}$ values also changes. For all the modulation schemes, convex imaging lens based receivers have higher $\tilde{d}_{\min, \mathbf{H}}$ values than that of non-imaging receivers. Thus at high

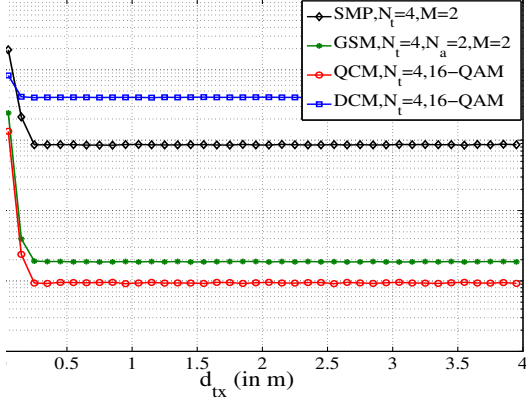


Fig. 7. BER performance of the convex imaging lens based receiver as a function of d_{tx} .

Receiver Structure	Receiver location	$\tilde{d}_{\min, \mathbf{H}}$			
		SMP	GSM	QCM	DCM
Non-imaging receiver	(0,0,0.5)	0.0007	0.0377	0.0413	0.0328
	(1,1,0.5)	0.0168	0.0370	0.0212	0.0296
	(1.5,-1.5,0.5)	0.0096	0.0164	0.0113	0.2990
	(-2,0,0.5)	0.0035	0.0056	0.0089	0.1841
Convex lens based imaging receiver	(0,0,0.5)	1.8952	2.6808	2.6822	0.8027
	(1,1,0.5)	0.4540	0.8238	0.9080	0.8025
	(1.5,-1.5,0.5)	0.4735	0.6755	0.9471	0.6192
	(-2,0,0.5)	0.4688	0.5967	0.9377	0.2118

TABLE II
 $\tilde{d}_{\min, \mathbf{H}}$ VALUES FOR SMP, GSM, QCM, AND DCM USING NON-IMAGING AND CONVEX LENS BASED IMAGING RECEIVERS.

SNRs, the BER performance of imaging lens based receiver is better than the non-imaging receiver. The maximum $\tilde{d}_{\min, \mathbf{H}}$ value at a given receiver location is shown in bold numbers and the corresponding modulation scheme is the best performing scheme at that receiver location.

Spatial distribution of best performing MIMO scheme: In this subsection, we present the best performing MIMO scheme among SMP, GSM, QCM, and DCM at various receiver locations based on their $\tilde{d}_{\min, \mathbf{H}}$ values. At a given receiver location, we obtain the channel gain matrix and then compute $\tilde{d}_{\min, \mathbf{H}}$ values using (8) for all the considered MIMO schemes. The best performing MIMO scheme at that receiver location is the scheme with the maximum $\tilde{d}_{\min, \mathbf{H}}$. To obtain the spatial distribution of the best performing MIMO scheme, the receiver plane located at a height of 0.5m above the floor is divided into a grid of 200×200 points. Each grid point is considered as a receiver location for simulation. At every receiver location, $\tilde{d}_{\min, \mathbf{H}}$ is computed for all the four MIMO schemes. Each modulation scheme is assigned a particular color; in the spatial distribution plot, the grid point is filled with the color of the best performing modulation scheme. This process is repeated for all the receiver locations across the room. The spatial distribution plot of the best performing MIMO scheme obtained in the case of non-imaging and convex imaging lens based receivers are shown in Figs. 8 and 9, respectively. In the case of non-imaging receiver, for the system parameters considered, DCM and QCM are the most favorable and second most favorable schemes across the room as they cover 50.1% and 20.7% of the room area. SMP and GSM perform best

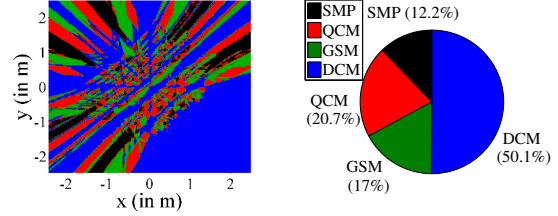


Fig. 8. Spatial distribution of best performing MIMO scheme among SMP, GSM, QCM, and DCM for the non-imaging receiver.

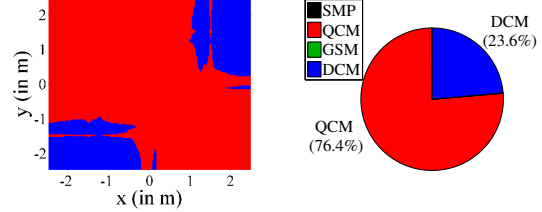


Fig. 9. Spatial distribution of best performing MIMO scheme among SMP, GSM, QCM, and DCM for the convex lens based imaging receiver.

across 12.2% and 17% of the room, respectively. In the case of convex imaging lens based receiver, QCM is the most favorable scheme as it performs best across 76.4% of the room; DCM is the next most favorable scheme as it performs best across 23.6% of the room. SMP and GSM are not the best performers with convex lens based imaging receivers.

V. CONCLUSIONS

We investigated the effect of using a convex lens based imaging receiver on the BER performance of state-of-the-art MIMO modulation schemes such as GSM, QCM, and DCM, in comparison with that of the well known SMP scheme. Because of the spatial decorrelation achieved by the convex lens, the imaging receiver was able to achieve significantly better performance (up to 68 dB at 10^{-5} BER) compared to a non-imaging receiver. Among the considered MIMO modulation schemes with imaging receiver, QCM and DCM outperformed GSM and SMP, and achieved the best spatial performance.

REFERENCES

- [1] H. Elgala, R. Mesleh, and H. Haas, "Indoor optical wireless communication: potential and state-of-the-art," *IEEE Commun. Mag.*, vol. 49, no. 9, pp. 56-62, Sep. 2011.
- [2] T. Fath and H. Haas, "Performance comparison of MIMO techniques for optical wireless communications in indoor environments," *IEEE Trans. Commun.*, vol. 61, no. 2, pp. 733-742, Feb. 2013.
- [3] R. Mesleh, H. Elgala, and H. Haas, "Optical spatial modulation," *IEEE/OSA J. Opt. Commun. New.*, vol. 3, no. 3, pp. 234-244, Mar. 2011.
- [4] S. P. Alaka et al., "Generalized spatial modulation in indoor wireless visible light communication," *Proc. IEEE GLOBECOM'2015*, Dec. 2015.
- [5] T. Lakshmi Narasimhan, R. Tejaswi, and A. Chockalingam, "Quad-LED and dual-LED complex modulation for visible light communication," *online: arXiv:1510.08805v3 [cs.IT]* 24 Jul 2016.
- [6] L. Zeng et al., "High data rate multiple input multiple output (MIMO) optical wireless communications using white LED lighting," *IEEE J. Sel. Areas Commun.*, vol. 27, no. 9, pp. 1654-1662, Dec. 2009.
- [7] T. Q. Wang et al., "Analysis of an optical wireless receiver using a hemispherical lens with application in MIMO visible light communications," *J. Lightw. Technol.*, vol. 31, no. 11, pp. 1744-1754, Jun. 2013.
- [8] P. Butala et al., "Performance of optical spatial modulation and spatial multiplexing with imaging receiver," *Proc. IEEE WCNC'2014*, Apr. 2014.
- [9] T. Chen, L. Liu, B. Tu, Z. Zheng, and W. Hu, "High-spatial-diversity imaging receiver using fisheye lens for indoor MIMO VLCs," *IEEE Photonics Lett.*, vol. 26, no. 22, pp. 2260-2263, Nov. 2014.